

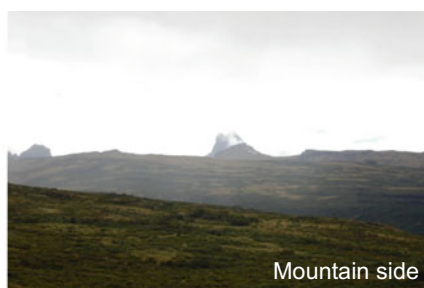
Climatology: Seasonal Changes of Rainfall Around Mount Kenya and Its Relation to Atmospheric Circulation



Wataru Morishima



Foothills side



Mountain side

Date: 2016/8/14 Cloud cover over the western slope of Mount Kenya during the dry season. Precipitation is predominant mostly in the afternoon

Abstract The regions surrounding Mount Kenya have both long and short rainy seasons, and the corresponding peak rainfalls occur during April and November, respectively. Rainfall in these two seasons reach their maximum potential in areas centered on the southeastern part of the foothills of Mount Kenya and in the Aberdare Range. The relationships between the onset of these rainy seasons and the inland penetrations of the easterly winds at 700 hPa demonstrated that during the long rainy season, wind penetration from the Indian Ocean occurs along the ridge, extending northwards from the southern hemisphere along the eastern coast. During the short rainy season, wind penetration occurs with the strengthening of easterly winds associated with deepening low pressure in the Congo Basin. The relationship between the location of the convergence and divergence of wind field at 700 hPa and the seasonal march of rainfall around Mount Kenya suggest that the seasonal changes in rainfall are not only a result of north–south movement of the convergence zone with the meridional component of wind, but also a result of east–west movement of the divergence zone with the zonal component of wind.

W. Morishima (✉)

Department of Geography, College of Humanities and Sciences, Nihon University, Sakurajyosui 3-25-40, Setagaya 156-8550, Tokyo, Japan
e-mail: morishima.wataru@nihon-u.ac.jp

Keywords Rainy season · Dry season · Convergence zone · Equatorial trough · Subtropical ridge · Zonal wind

1 Introduction

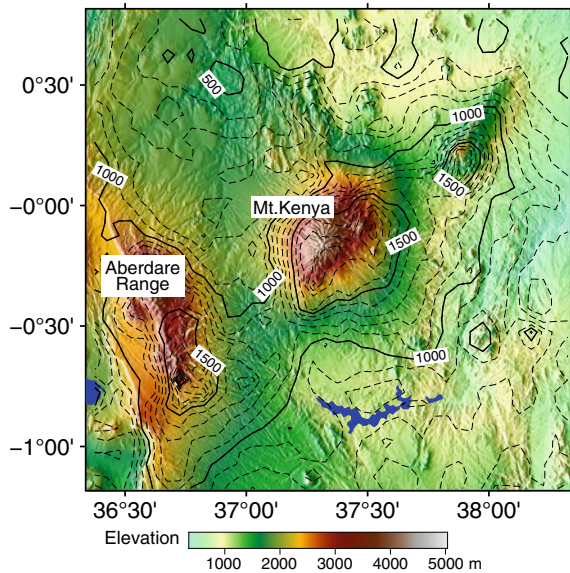
Rainfall in the equatorial regions of East Africa, where Mount Kenya is located, is characterized by bimodal seasonal variations. The long rainy season occurs between March and May, and the short rainy season occurs between October and November. The spatial distribution of rainfall strongly depends on regional topography (Oettli and Camberlin 2005). As rainfed cultivation depends on these seasons, any changes in the amount and duration of rainfall during these seasons have a significant impact on agricultural production. Based on precipitation data at observation stations, several previous studies have elucidated the long-term variability of precipitation in different areas, including the equatorial region of East Africa. According to Nicholson et al. (2018), the annual rainfall in this region has remained highly variable since the late nineteenth century, although there is no significant trend of it. Seasonal rainfall in the long rainy season displays a distinct trend of dryness since the early 1970s, while the short rainy season exhibits a wetting trend since the 1960s, indicating a major change in regime (Funk et al. 2005, 2008; Williams and Funk 2011).

Nicholson (2017) provided a comprehensive review on the variability of rainfall in East Africa. In equatorial East Africa, the interannual variabilities of rainfall appear relatively coherent; however, if more detailed information is desired for the long rainy season, we should consider the coastal, the western highlands, and the regions around Lake Victoria separately. Yang et al. (2015) have also mentioned the need to fully understand the seasonal changes of climatological rainfall, because the results of recent coupled models overestimate rainfall in the short rainy season and misrepresent the seasonal changes in East Africa. In this study, the authors have shown that the atmosphere over a region with bimodal seasonal change of rainfall remains convectively stable throughout the year, and the divergence in the lower troposphere contributes to dryness in the region. It has also been demonstrated that enhanced rainfall during the two rainy seasons occurs due to increase in the static energy of surface moisture and vertically integrated moisture flux (Yang et al. 2015). On the other hand, several studies have shown that seasonal and interannual variations of zonal winds in the middle troposphere are related to variations in rainfall during the wet and dry seasons (e.g. Nakamura 1968). It is suggested that at a pressure of 700 hPa in western Kenya, an increase and decrease of rainfall over the highlands during boreal summer are associated with westerly and easterly wind anomalies, respectively, and a reverse relationship exists in coastal areas (Camberlin 1996). Furthermore, Camberlin and Wairoto (1997) demonstrated that rainfall in the central highlands near Nairobi tends

to decrease during the long rainy season, and increase during the short rainy season. Similar trend can be observed in easterly wind anomalies.

The objective of this study is to understand the characteristics of mean seasonal changes and the spatial distribution of rainfall around Mount Kenya. Using data with high temporal and spatial resolution, we attempted to demonstrate the linkage of these seasonal characteristics with large-scale atmospheric circulation. Data from the Climate Hazards Group InfraRed Precipitation with Station (CHIRPS) were used in this study. CHIRPS provides an estimated dataset for precipitation based on satellite infrared data and ground precipitation (Funk et al. 2015). These data, with a spatial resolution of 0.05° , spatially cover the land area between the northern and southern latitudes of 5° , and temporally, from 1981 to the present. In this analysis, the total data of pentadal precipitation (i.e., five-day rainfall with six pentads per month) were used for a period of 38 years from 1981 to 2018; an area of approximately 200 km^2 , with 40 east–west (36.375°E – 38.375°E) and 40 north–south (1.175°S – 0.775°N) grids centered on Mount Kenya, was covered, as shown in Fig. 1. The JRA-55 Product, provided from the Japanese 55-year Reanalysis project carried out by the Japan Meteorological Agency, was used to investigate the relationship between seasonal changes in rainfall and atmospheric circulation. The analyzed data has a spatial resolution of 1.25° latitude/longitude. The pentad datasets were also created for the geopotential height and wind data at 850 and 700 hPa from 1981 to 2018 to match the precipitation dataset. Data from NASA’s Shuttle Radar Topography Mission (SRTM) and United States Geological Survey (USGS)’s Global 30 Arc-Second Elevation (GTOPO30) were used for generating large- and small-scale maps to show the topography.

Fig. 1 Mean annual rainfall in the study area. Contour interval for rainfall is 100 mm. Shuttle Radar Topography Mission (SRTM) data are used for terrain representation



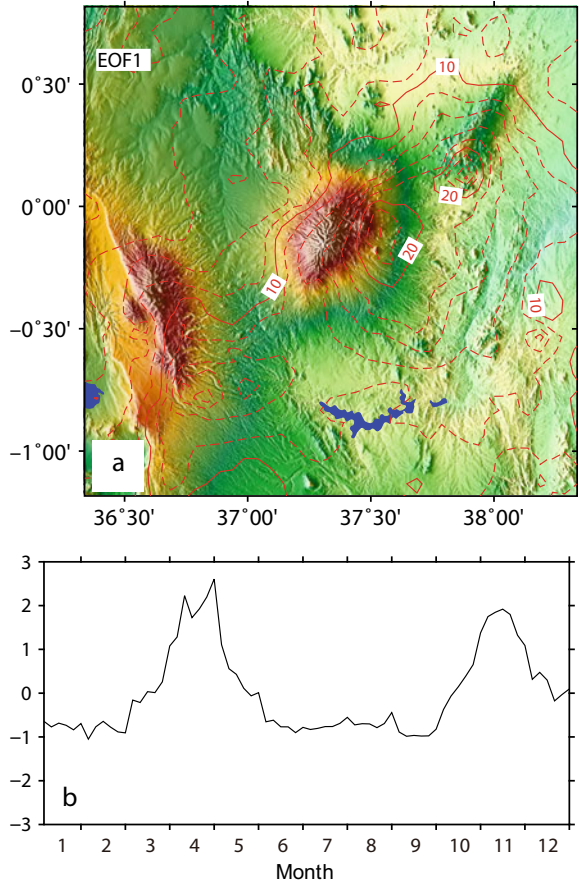
2 Rainfall Distribution and Its Seasonal Changes Around Mount Kenya

Figure 1 shows the distribution of the mean annual rainfall during the period 1981–2018. The calculations were made using CHIRPS data. It was found that the rainfall over Mount Kenya and the Aberdare range exceeds 1000 mm, and that over the southern to southeastern foothills of these mountains exceeds 1500 mm. The spatial characteristics of rainfall around Mount Kenya was in good agreement with that obtained from ground-based observations by Thompson (1966). However, the spatial resolution of the CHIRPS data was not high enough to represent the decrease in rainfall near the summit.

To reveal the average seasonal changes in rainfall distribution, the empirical orthogonal function (EOF) analysis was applied to the correlation matrix derived from 72 mean pentad rainfalls from 1981 to 2018 for a total of 1600 grids, with 40 east–west and 40 north–south grids, as shown in Fig. 1. The results indicate that the first and second EOFs can explain 81.4% and 10.4% of the seasonal variations, respectively. Their total contribution of more than 90% suggest that these two components were the most representative characteristics of the seasonal variations in rainfall.

Figure 2 shows the time coefficient of the first EOF (EOF1) and the spatial pattern of the corresponding regression coefficients for the pentad rainfall. The regression coefficients were found to have positive signs in all areas, and their relationship with time coefficients indicate that EOF1 was extracted as the seasonal mode of rainfall with wet and dry conditions in the entire area. The factor loadings values of higher than 0.8 (not shown in the figure) indicate a statistically significant relationship ($p < 0.01$) across the region, except for the western side of the northern hemisphere at 36.5°E. In fact, a correlation coefficient of 0.95 was obtained between the time coefficients of EOF1 and the total pentad rainfall over the entire region. It was also found that the eastern foothills of Mount Kenya and the southern Aberdare Range are situated in areas of greater rainfall variations with values above 20 mm, while the western foothills of these mountains experience lesser variations. These distributions, which are similar to those of the annual rainfall given in Fig. 1, can be considered as an effect of the mountain on wind flowing along southeast-to-east direction. This explains why rainfall is higher on the windward side and lower on the leeward side. This spatial pattern of rainfall is reflected by changes in the time coefficients. Upon comparing the rainfall distribution in individual pentads with time coefficient, the spatial pattern of EOF1 was clearly observed during the period of “long rains” that occurred from late March to mid-May. On the other hand, periods of “short rains” occurred from middle October to middle December. The time coefficients indicated that the peak rainy seasons occurred during mid to late April and early to mid-November; thereafter, they decreased from the beginning of May and from mid-November, respectively. On the other hand, the spatial distribution of regression coefficients for the second EOF (EOF2) demonstrated that the positive values tend to appear at relatively high elevations, and negative values at low elevations (Fig. 3).

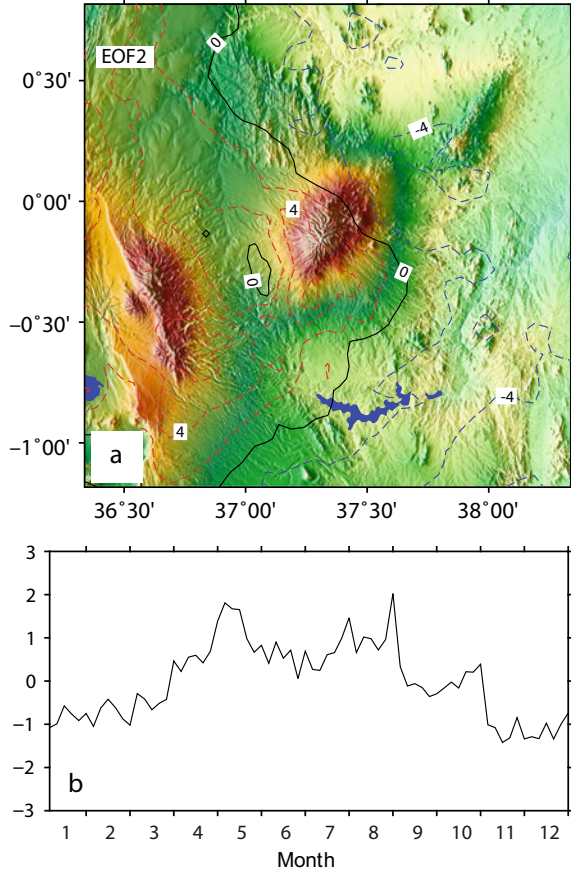
Fig. 2 **a** The spatial pattern, and **b** the time coefficients for the first empirical orthogonal function (EOF; EOF1) detected from 72 pentad rainfalls. **(a)** Distribution of regression coefficient for the pentad rainfall in relation to time coefficient. The contour interval is 2 mm per unit. Shuttle Radar Topography Mission (SRTM) data are used for terrain representation



However, significant factor loadings ($p < 0.01$) were found only in the positive areas, which extend northwestward from the southern foot of Mount Kenya and northward from the southern part of the Aberdare Range. Overall, we can consider EOF2 as an expression of rainfall variation at high elevations. As the time coefficients increase from the end of the rainy season (May) to August, the high elevation areas and their northward regions display an increasing trend of rainfall during this period.

Classifying the seasonal changes in rainfall distribution pattern based on temporal changes of the time coefficient for two EOFs, the seasonal progress of rainfall can be recognized not only from the two rainy and dry seasons but also from those seasons occurring during the transitional periods between the rainy and dry seasons. The pentad rainfall distributions are shown as typical instances of seasonal rainfall in Fig. 4. From middle December (70th pentad) to middle March (14th pentad), the time coefficients of both the first and second EOF components displayed negative values, indicating low rainfall over the entire region (Fig. 4a). After this dry season, the time coefficients for EOF1 started to have positive values from middle March

Fig. 3 Same as Fig. 2, but for the second empirical orthogonal function (EOF; EOF2)



to late March (15th–17th pentad), while those for EOF2 remained negative. This combination of time coefficients reflects a situation in which rainfall increases over the entire region, although it is less pronounced in the southern foothills of the mountains and in higher elevation areas (Fig. 4b). After this transitional period, precipitation during “long rains” season occurred in full swing over the entire region with positive time coefficients of EOF1 and EOF2, and it lasted from the end of March (18th pentad) to the end of May (30th pentad). In particular, the rainfall pattern of EOF2 was remarkable during early to middle May, with increased rainfall in high-altitude areas such as the southern skirts of Mount Kenya (Fig. 4c). The rainfall distribution characterized by the spatial pattern of EOF2 occurred during the dry season from early June (Fig. 4d) and continued until early October. The time coefficient of EOF1 began to increase during middle October, which increased the rainfall in the low-altitude areas (Fig. 4e). In comparison with the prior dry season from January to February, this dry season can be distinguished by the amount of rainfall in high altitudes. During the short rainy season from middle October to

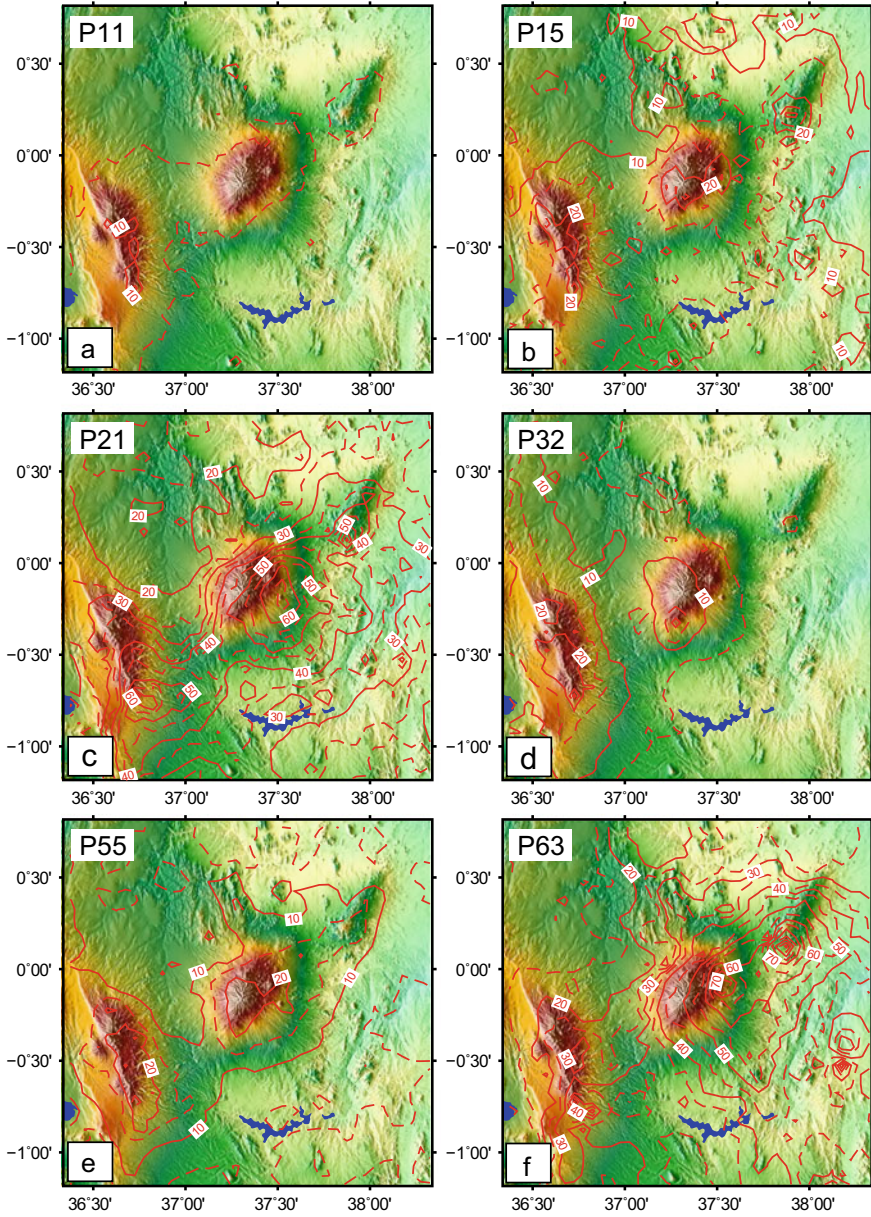


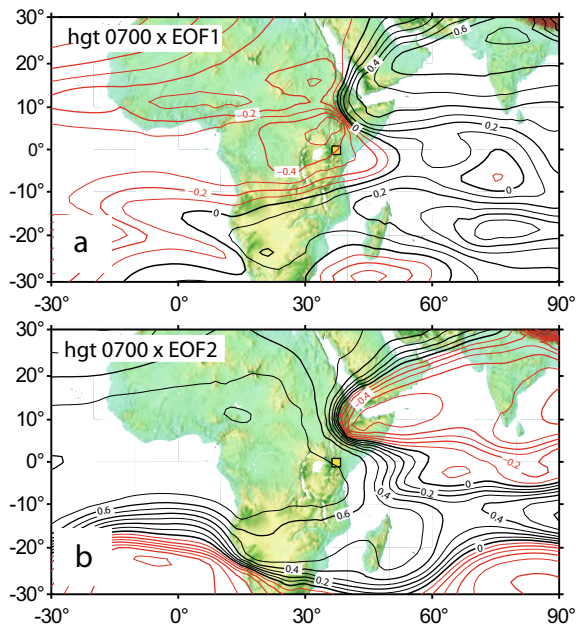
Fig. 4 Seasonal changes in rainfall distribution. Contour interval for rainfall is 5 mm. The alphabets from **a** to **f** in each figure denote the 11th, 15th, 21st, 32nd, 55th, and 63rd pentads, respectively. Shuttle Radar Topography Mission (SRTM) data are used for terrain representation

middle December (Fig. 4f), the time coefficient of the EOF2 became negative, and that of EOF1 was positive. Comparing the rainfall distributions of long and short rainy seasons (Fig. 4c, f), it is observed that the only difference in distribution of rainfall during these rainy seasons is that there is no significant increase of rainfall at the southern foot of the mountains during the short rainy season.

3 Relationship Between Seasonal Changes in Rainfall and the Atmospheric Circulation Field

As seen in the previous section, the seasonal changes in the distribution of rainfall around Mount Kenya are indicated by two EOF modes of seasonal changes, one of which is almost similar in all areas from low to high-altitude areas, and the other is limited to high-altitude areas. To consider the relationship between the characteristics of these seasonal changes and the large-scale atmospheric circulation, a correlation analysis was conducted between the time coefficients of each EOF and the geopotential height. Considering that the elevation above 1500 m covers a wide are, including the study area, the relationships at 700 hPa were plotted (Fig. 5). EOF1 had a significant negative correlation ($p < 0.01$) in the equatorial interior of the African continent, and a significant positive correlation in regions extending from the Indian subcontinent to the northern part of the Horn of Africa and at approximately 20°S over the southern Indian Ocean (Fig. 5a). This suggests that the increase in rainfall

Fig. 5 Spatial patterns of correlation coefficients between the geopotential heights at 700 hPa and the time coefficients detected from the empirical orthogonal function (EOF) analysis for rainfall. **a** and **b** show the relations to time coefficients for EOF1 and EOF2, respectively. The yellow box corresponds to the area in Fig. 1. Global 30 Arc-Second Elevation (GTOPO30) data are used for terrain representation



for EOF1 occurred concurrently with i) a decrease in atmospheric pressure at the northern side of the study area, and ii) an increase in atmospheric pressure over the Indian subcontinent and the southern Indian Ocean. Corresponding to these changes, a zonal low-pressure area appeared in the equatorial region of the African continent, while high-pressure areas were clearly visible in the Indian subcontinent and in the South Indian Ocean. On the other hand, for EOF2, the negatively correlated area was distributed in east–west direction from the Indian subcontinent to the northern Horn of Africa, while the positively correlated area appeared over the equatorial region of Africa, and extended to Madagascar (Fig. 5b). The positive and negative time coefficients of EOF2 corresponded to the periods when low pressure, associated with the Indian monsoon, extended from the Indian subcontinent to the northern Horn of Africa, and when the same area was covered by the subtropical anticyclone, respectively. In addition, we considered that the positively correlated region over Africa corresponds to the development of a subtropical anticyclone in boreal summer and the expansion of the low-pressure area from the equator during winter.

To understand these relationships between rainfall distribution and geopotential heights from the standpoint of seasonal changes in pressure fields and the associated wind flows, the geopotential height and wind flow at 700 hPa for the same pentads of Fig. 4 were plotted (Fig. 6). The same analysis was also performed at 850 hPa field; however, the results are not shown in the figure.

It was found that during dry season, mainly in January and February, the ridge extended from the northern hemisphere along the eastern shore of Africa to the southern hemisphere, and the northeasterly airflow extended to the southern hemisphere (Fig. 6a). On the other hand, at 850 hPa and at the same time, a low-pressure zone developed at the north of Lake Victoria and a ridge formed from the northern hemisphere, which extended along the eastern coast of Africa. Due to this pressure pattern, northeasterly winds near the Horn of Africa changed to easterly winds towards Lake Victoria near the equator. The easterly winds tended to diverge to the north and to the south around the equatorial area of research interest.

From the 13th pentad (early March), the ridge extending from the northern to southern hemisphere began to retreat to the northern hemisphere. On the 15th pentad, the study area became an obscure high-pressure area that formed between the low-pressure areas over the West African and Indian Ocean equatorial regions (Fig. 6b). In the southern hemisphere, another ridge began to form along the eastern coast of the African continent from the south to the equator. Corresponding with this ridge expansion, the weak convergence of northerly and southerly wind components appeared along 10°S near the coast of Africa. Furthermore, over the ocean near the east coast of Africa (7.5°S, 40°E), the wind diverged to the east and west directions. This area, where such convergence of the north–south components and divergence of the east–west components of the wind occurred was referred as the EWdNSc area (denoted as a circle in Fig. 6). The seasonal changes in wind direction around Mount Kenya appeared to change with the movement of this area, which was related to seasonal pressure distribution. In the 15th pentad, when this area was in the southern hemisphere, the wind direction around Mount Kenya continued to be northeasterly. At 850 hPa, easterly winds toward Lake Victoria still prevailed around the research

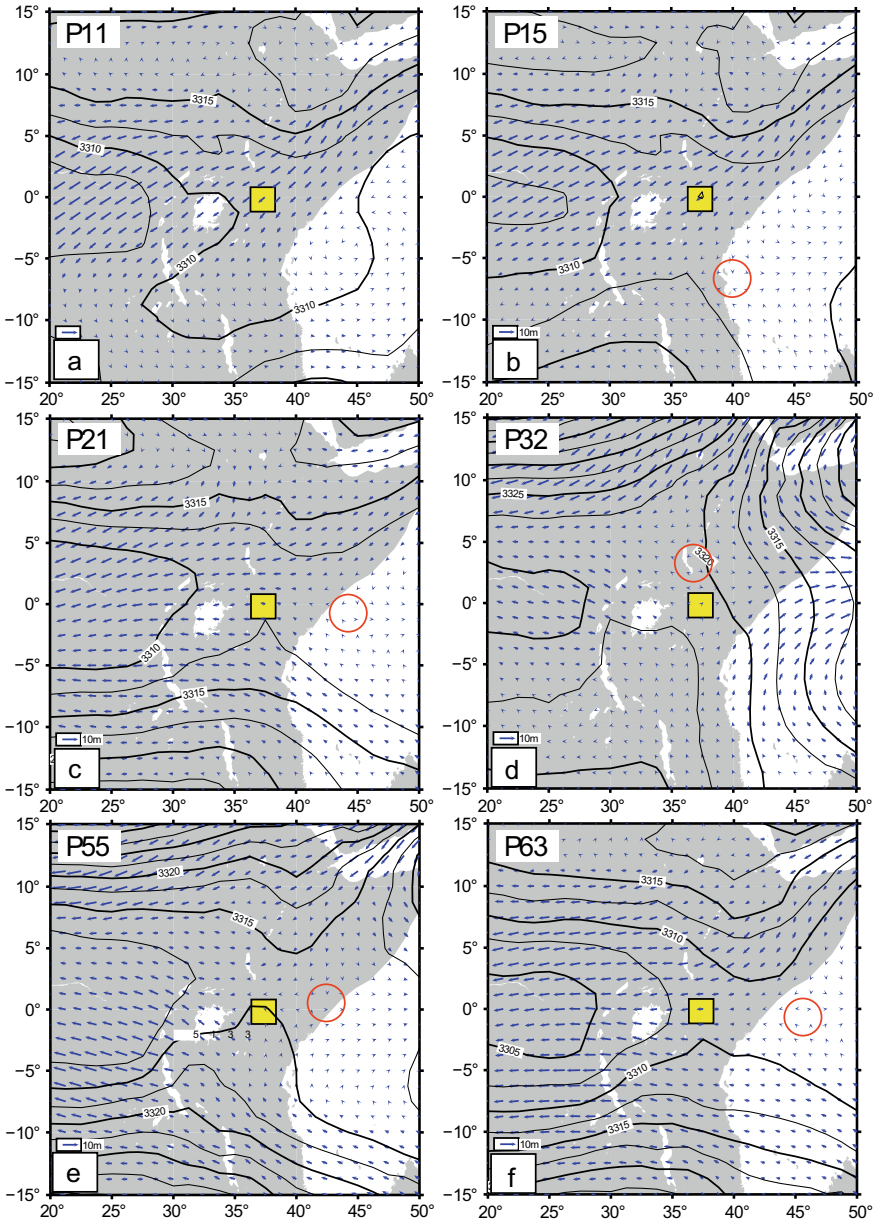


Fig. 6 Seasonal characteristics of geopotential heights and wind fields at 700 hPa. The letters from “a” to “f” in each figure denote the 11th, 15th, 21st, 32nd, 55th, and 63rd pentads, respectively. The red circle and yellow box show the location of EWdNSc area and the study area for rainfall, respectively

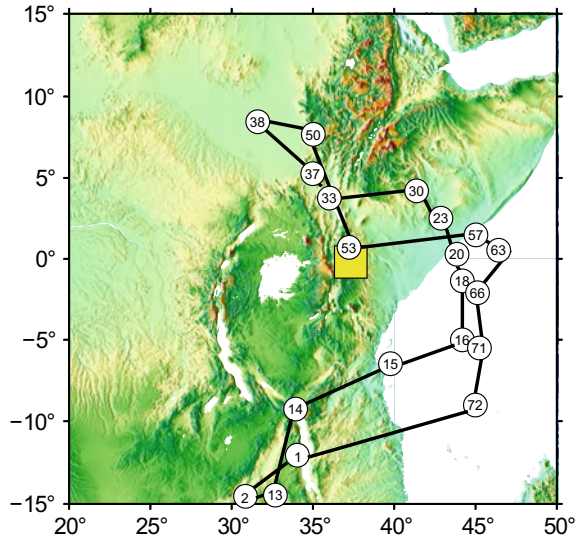
area; however, similar to conditions at 700 hPa, a ridge extension occurred over the eastern coast of the continent from the southern hemisphere, and a southerly wind component began to appear over the southern hemisphere. With the strengthening of the southerly component, the divergence of north and south wind components around Mount Kenya were weakened. This might have contributed to the onset of the rainy season around Mount Kenya.

After mid-March, the low-pressure area around Lake Victoria became gradually obscured at 850 hPa, and was replaced by a low-pressure area over the western part of the Ethiopian Plateau. Along with this replacement, the ridge extended northwards from the southern hemisphere along the east coast of the continent and reached the equator. In the middle of April, it crossed the equator and expanded to the northern hemisphere. The changes in the pressure field at 700 hPa were synchronized with those at 850 hPa. This involved ridge extension from the southern hemisphere to the north, and northeastward trough extension from the vicinity of Lake Victoria to the western Ethiopian Plateau was clearly visible (Fig. 6c). As the wind direction around Mount Kenya shifted from northeasterly to southeasterly direction at 700 hPa, the formations of the ridge in the southern hemisphere and of the trough in the northern hemisphere facilitated the entry of southeasterly winds from the South Indian Ocean to the equatorial interior. These southeasterly and northeasterly winds from the ridge were maintained at the south of the Horn of Africa and converged near the equator. Moreover, the extension of the ridge from the southern hemisphere also contributed to the formation of the EWdNSc area near the east coast of the continent at the equator, which brought easterly winds from the ocean.

The EWdNSc area moved to Lake Turkana in early June (Fig. 6d), and the winds around Mount Kenya shifted from southeastern to southwestern direction. In other words, the movement of the EWdNSc area appeared both with the northward shift of convergence line by northerly and southerly wind components, and with the westward shift of divergence area with easterly and westerly wind components. This movement of the EWdNSc area might be considered a result of the westward movement of the relative ridge, formed between the troughs extending from the Congo Basin, and from the Horn of Africa. Such trough expansion from the Horn of Africa could be related to the deepening and westward expansion of the low-pressure system in the North Indian Ocean. In a follow-up confirmation of the seasonal changes in rainfall around Mount Kenya associated with the movement of the EWdNSc area, the area moved to the north of Mount Kenya in early June, which corresponds to the beginning of the dry season around Mount Kenya. It continued to be located at the northwestern side of Mount Kenya for the period characterized by low rainfall and the prevalence of southwesterly winds until the middle of September. This period of prevailing southwesterly winds also corresponded with the positive phase of EOF2, which predominates the mountain-centered rainfall, although the amount is relatively small.

The trough in the North Indian Ocean side receded rapidly in middle September, while the ridge distinctively appeared along the eastern coast from the northern hemisphere side. The EWdNSc area, which was located on the western side of the Ethiopian Plateau in early September, moved southwards to the north side of

Fig. 7 Seasonal migration of the EWdNSc area. The numbers inside the circles denote the pentad number. The yellow box shows the study area considered for rainfall estimation. Global 30 Arc-Second Elevation (GTOPO30) data are used for terrain representation



Mount Kenya in middle September, and thereafter moved eastward along the equator (Figs. 6e and 7). This can be also referred to as the beginning of the short rainy season, when the easterly winds became dominant around Mount Kenya. Subsequently, as the low pressure deepened on the Congo Basin side, the easterly winds became even stronger, which resulted in the maximal period of short rainy season (Fig. 6f). The wind direction changed from the east to northeast as the ridge moved from the northern to the southern hemisphere, and the rainy season terminated in late December (Fig. 6).

4 Seasonal Changes in Rainfall in the Context of the EWdNSc Area Movement

As shown in Sect. 3, the seasonal changes in rainfall pattern around Mount Kenya coincide with the seasonal expansion and contraction of the ridges from the two hemispheres along the east coast, and with the expansion and contraction of the troughs over the Congo Basin and over the North Indian Ocean at 700 hPa. The easterly wind component around Mount Kenya at 850 hPa remained active throughout the year, although the northerly and southerly components changed seasonally. With the seasonal changes of these ridges and troughs, the convergence zone associated with the meridional components of winds moved in north–south direction. This convergence zone also had divergence zones of zonal wind components, which formed the boundary of troughs distributed over the Congo Basin and the Indian Ocean. In this study, the divergence area of zonal wind components, formed in the convergence zone of meridional wind components, has been referred to as the EWdNSc area. It was

observed that the location of the EWdNSc area is related to the changes in the zonal wind components around Mount Kenya. Its location in the equatorial Indian Ocean is considered to be important in promoting the inland penetration of easterly winds from the Indian Ocean, especially during the rainy season. In addition, the inland movement of the EWdNSc area during dry season in boreal summer was consistent with the changes in the wind components from easterly to westerly around Mount Kenya. This movement might explain the mechanism behind the dominance of the westerly winds, as pointed out in previous studies (Nakamura 1968).

The relationship between the seasonal march of the EWdNSc area and rainfall around Mount Kenya is explained and summarized in Fig. 7, where the pentad numbers required to trace the position of the EWdNSc area are shown. Around the middle of March (14th pentad), the expansion of the South African anticyclone to the equator became more pronounced, and the south wind flowing from Madagascar to the east coast of Africa invaded the northern part of Lake Malawi. The EWdNSc area situated in the southwest of the lake moved to its northern side. Concurrent with this movement, the time coefficient of rainfall for EOF1 increased. The EWdNSc area moved rapidly into the Indian Ocean towards the end of March due to the strengthening of the southeasterly winds from the South African High to the equator, and due to the eastward movement of the relative ridge between the equatorial troughs. This migration of the EWdNSc area caused the northeast and southeast winds to converge around Mount Kenya, which corresponded with a full-fledged rainy season. The EWdNSc area continued to remain in the east of Mount Kenya until late May (30th pentad), which brought easterly winds from the Indian Ocean. Subsequently, it gradually moved to the northwest. From early to mid-June (32nd pentad), when the South African High expanded further north and got associated with the Arabian High or the Sahara High, a north–south ridge was formed at approximately 30°E. Subsequently, the EWdNSc area migrated rapidly westwards to the northwestern side of Mount Kenya, and the long rainy season terminated. As the EWdNSc area was located to the west of Mount Kenya until late September (53rd pentad), the southwesterly wind blowing from the inland prevailed around Mount Kenya at 700 hPa. During this period, rainfall became more pronounced on the high-altitude side, which was reflected in the spatial distribution of EOF2. In relation to the geopotential height at 700 hPa (Fig. 5b), this southwesterly wind could be also a result of widespread increase in pressure over the equatorial region and a drop in pressure over the northern Horn of Africa. After late September, the time coefficient of EOF1 began to increase again; however at this time, the EWdNSc area shifted to the southeast and stayed to the east of Mount Kenya attracting the easterly wind from the ocean. Subsequently, the EWdNSc area migrated eastwards along the equator until the middle of November (63rd pentad), when the short rainy season reached its peak. The equatorial trough on the Congo Basin side also deepened, and easterly winds became stronger. From late November, the EWdNSc area migrated southwards along the meridian at 45°E to approximately at 10°S by the end of December. As the location of the north–south convergence zone moved southward, the short rainy season was gradually terminated. In the beginning of January, the EWdNSc area moved from the Indian Ocean to Lake

Malawi, and subsequently, it migrated southwards to stay in the southwestern side of Lake Malawi until late February.

5 Summary

In this chapter, the characteristics of seasonal changes in rainfall around Mount Kenya were studied, and the relationship between the changes in the atmospheric circulation field and the rainy and dry seasons were evaluated. Most of the seasonal changes in rainfall distributions in the area appeared to be related to the overall rainfall, and in the mountainous areas, the changes corresponded to rainy and dry seasons. The investigation of the characteristics of wind directions around Mount Kenya at the onset, peak, and withdrawal stages of the rainy and dry seasons confirmed that the wind direction at 850 hPa remained easterly throughout the year, while the wind direction at 700 hPa showed a characteristic change. The easterly winds at 700 hPa were predominant in both rainy seasons, while the northeasterly winds were predominant in the dry season, followed by the short rainy season. The southwesterly winds were dominant in the dry season followed by the long dry season. Both the dominant wind directions in the dry season originated from the land. On the other hand, during the dry season corresponding to boreal summer, an additional seasonal component was detected as EOF2 for rainfall, suggesting that the increase in rainfall was mostly associated with southwesterly winds. In the rainy season, the easterly winds brought the oceanic air from the Indian Ocean to inland. It is evinced that the north–south movement of the convergence zone, formed by northerly and southerly wind at 700 hPa, is an important parameter for the seasonal changes of rainfall in this region. However, the ridge between the continental and oceanic equatorial troughs determines the flow of oceanic and continental winds and the amount of water vapor produced, whereby the location of the ridge to the east of the target area strengthens the flow of oceanic winds.

References

- Camberlin P (1996) Intraseasonal variations of June–September rainfall and upper-air circulation over Kenya. *Theor Appl Climatol* 115(3–4):107–115
- Camberlin P, Wairoto J (1997) Intraseasonal wind anomalies related to wet and dry spells during the “long” and “short” rainy seasons in Kenya. *Theor Appl Climatol* 58(1–2):57–69
- Funk C, Dettinger MD, Michaelsen JC, Verdin JP, Brown ME, Barlow M, Hoell A (2008) Warming of the Indian Ocean threatens eastern and southern African food security but could be mitigated by agricultural development. *Proc Natl Acad Sci USA* 105:11081–11086
- Funk C, Senay G, Aswaw A, Verdin J, Rowland J, Korecha D, Eilerts G, Michaelsen J, Amer S, Choularton R (2005) Recent drought tendencies in Ethiopia and equatorial-subtropical eastern Africa. In: *Famine early warning system network special report*, US Agency for International Development

- Funk C, Peterson P, Landsfeld M, Pedreros D, Verdin J, Shukla S, Husak G, Rowland J, Harrison L, Hoell A, Michaelsen J (2015) The climate hazards infrared precipitation with stations—A new environmental record for monitoring extremes. *Sci Data* 2:150066. <https://doi.org/10.1038/sdata.2015.66>
- Nakamura K (1968) Equatorial westerlies over East Africa and their climatological significance. *Geogr Rev Japan* 41:359–373
- Nicholson SE (2017) Climate and climatic variability of rainfall over eastern Africa. *Rev Geophys* 55:590–635
- Nicholson SE, Funk C, Fink AH (2018) Rainfall over the African continent from the 19th through the 21st century. *Glob Planet Change* 165:114–127
- Oettli P, Camberlin P (2005) Influence of topography on monthly rainfall distribution over East Africa. *Clim Res* 28:199–212
- Thompson BW (1966) Mean annual rainfall of Mount Kenya. *Weather* 21:48–49
- Williams AP, Funk C (2011) A westward extension of the warm pool leads to a westward extension of the Walker circulation, drying eastern Africa. *Clim Dyn* 37:2417–2435
- Yang W, Seager R, Cane MA, Lyon B (2015) The annual cycle of East African precipitation. *J Clim* 28(6):2385–2404